The magnetic coupling of a piezoelectric cantilever for enhanced energy harvesting efficiency

2010 Smart Mater. Struct. 19 045012

(http://iopscience.iop.org/0964-1726/19/4/045012)

Smart Mater. Struct. **19** (2010) 045012 (7pp) doi:10.1088/0964-1726/19/4/045012

The magnetic coupling of a piezoelectric cantilever for enhanced energy harvesting efficiency

Ji-Tzuoh Lin[1], **Barclay Lee**[2] **and Bruce Alphenaar**[1]

[1] Department of Electrical and Computer Engineering, University of Louisville, Louisville, KY 40292, USA
[2] Dupont Manual High School, Louisville, KY 40292, USA

Received 24 August 2009, in final form 27 January 2010
Published 25 February 2010
Online at stacks.iop.org/SMS/19/045012

Abstract
It is shown that the energy harvesting capabilities of a piezoelectric cantilever can be enhanced through coupling to a static magnetic field. A permanent magnet is fixed to the end of a piezoelectric cantilever, causing it to experience a non-linear force as it moves with respect to a stationary magnet. The magnetically coupled cantilever responds to vibration over a much broader frequency range than a standard cantilever, and exhibits non-periodic or chaotic motion. While the off-resonance response is substantially increased compared to that of a standard cantilever, no reduction in the response at the resonant frequency is observed, as long as a symmetric magnetic force is applied. The magnetically coupled cantilever motion is analyzed using a simple driven harmonic oscillator model with a non-linear magnetic force term. The results show that magnetic coupling can be used to increase the amount of power scavenged from environments containing multi-mode, or random vibration sources.

1. Introduction

Harvesting energy from background mechanical vibrations in the environment has been proposed as a possible method to provide power in situations where battery usage is impractical or inconvenient. The most commonly used method for energy harvesting is to generate power from the vibrations of a piezoelectric material [1–3]; other methods include electromagnetic inductive coupling [4–6] and charge pumping across vibrating capacitive plates [7–10]. It has been shown that a piezoelectric cantilever attached to a vibrating structure can be used to power wireless transmission nodes for sensing applications [9]. In order to generate sufficient power, the frequency of the vibration source must match the resonant frequency of the piezoelectric cantilever. If the source vibrates at a fixed, known frequency, the dimensions of the cantilever, and the proof mass can be adjusted to ensure frequency matching. Many naturally occurring vibration sources do not have a fixed frequency spectrum, however, and vibrate over a broad range of frequencies. Lack of coupling of the piezoelectric cantilever to the off-resonance vibrations means that only a small amount of the available power can be harvested.

Recent reports have shown that the resonant frequency of a simply supported beam [11] or a piezoelectric cantilever [12] can be tuned by applying an axial force. Research also show that the resonant frequency of a cantilever can also be manipulated by applying a transverse force on the cantilever [13, 14]. (In all these cases, the cantilevers response remained within the linear regime.) In principle, this effect could be developed into an active tuning scheme which matches the cantilever resonance to the maximum vibrational output of the environment at any particular time. Calculations indicate, however, that the power consumed by active tuning completely offsets any improvement obtained in the scavenging efficiency [15]. More promising are passive tuning schemes in which a fixed force modifies the frequency response of the cantilever beam, without requiring additional power input. For example, an attractive magnetic force acting above the cantilever beam reduces the spring constant of the cantilever and lowers the resonance frequency [13, 14], while an attractive force acting along the axis of the cantilever applies axial tension, and increases the resonance frequency [12]. While this can be used to tune the resonant frequency, there is no increase in output power, and the cantilever motion can even be dampened by the magnetic force and the resulting power output reduced [12, 13].

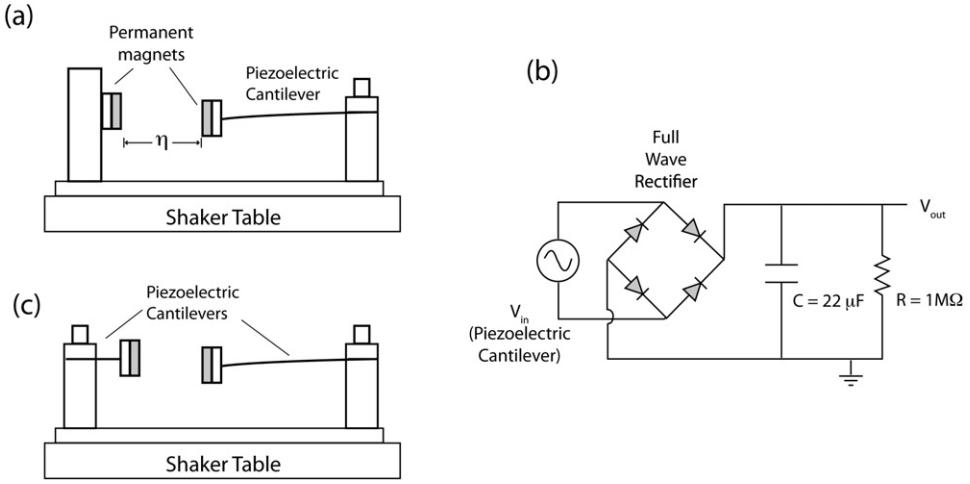

Figure 1. (a) Set-up with fixed opposing magnet. (b) Measurement circuit. (c) Set-up with opposing magnetic attached to a second cantilever.

The use of a magnetic force to introduce non-linear oscillation in cantilever motion has recently been reported [16–18]. A pendulum made with piezoelectric material [16] was used to study the energy output under different strengths of random Gaussian noise. An improvement of between 400% and 600% was observed compared to a standard linear oscillator. A piezomagnetoelastic structure [17] with two external magnets was studied, in which chaotic motion was observed outside the resonance frequency. It was further reported [18] that the softening response of a cantilever due to a magnetic attractor expands the response bandwidth and also increases the off resonant amplitude significantly.

Here, we show that by modifying the orientation and magnitude of the magnetic force, the frequency response of the piezoelectric cantilever can be substantially altered in a way that provides an effective method to harvest off-resonance vibrations. A fixed magnet is placed opposite the cantilever axis to introduce a small, non-linear force on either side of the equilibrium position. The magnetic force drops off with distance away from the equilibrium point, and so has only a minor influence at resonance where the cantilever deflection is relatively large. Outside the resonant frequency, the magnetic force causes the cantilever to undergo chaotic motion between the local minima on either side of the equilibrium point. The response is thus broadened by the appearance of non-periodic oscillations outside of the resonance condition, while the output at the resonant frequency remains unchanged. This provides an effective method to harvest off-resonance vibrations, and increase the output of the piezoelectric cantilever for random or broad-band vibration sources. We will compare the normal cantilever with the magnetic coupled cantilever in the non-linear regime with consideration of both the transverse forces and the axial forces.

2. Experiment

Figure 1(a) shows the set-up for the magnetically coupled piezoelectric cantilever measurements. The cantilever is manufactured using commercially available unimorph piezoelectric discs composed of a 0.09 mm thick PZT layer deposited on a 0.1 mm thick brass shim (APC International, MFT-50T-1.9A1). The disc is cut into a 13 mm wide by 50 mm long strip, and clamped at one end to produce a 44 mm long cantilever. The PZT layer extends 25 mm along the length of the cantilever, and the remainder is brass only. The proof mass (including the magnet and an additional fixture that holds the magnet) weighs 2.4 g, while the cantilever itself weighs 0.8 g. The electrical leads are carefully soldered with thin lead wires (134 AWP, Vishay) to the top side of the PZT and the bottom side of the shim. Vibration is generated by a shaker table (Labwork ET-126) powered by an amplified sinusoidal wave using a Yokogawa EG300 function generator and a Labwork Pa-13 amplifier. A custom Labview data acquisition program measures output voltage from the cantilever beam. A 5 mm diameter disc-shaped rare earth magnet (Radio Shack model 64-1895) is attached to the vibrating tip of the cantilever beam, while an opposing magnet of the same type is attached directly to the shaker table frame. In all measurements, the shaker table acceleration is set to approximately 7 m s^{-2}, and the frequency swept from 0 to 50 Hz in 0.5 Hz steps. The opposing magnet fitted at the free end of the cantilever supplies a symmetrical, repulsive force about the balance of the cantilever during vibration. The horizontal separation between the magnets (designated by η) is adjusted to be approximately $\eta = 5$ mm. This separation is found to provide the best compensation for the spring force, and makes the effective restoring force as small as possible near the equilibrium point.

Figure 2(a) shows the output of the cantilever as a function of shaker table vibration frequency for the case where the opposing magnet is fixed to the shaker table. The voltage generated by the piezoelectric cantilever beam is rectified, and detected across a 22 μF capacitor and 1 MΩ resistor in parallel, using the circuit shown in figure 1(b). The results from two measurement runs in the coupled state are shown, together with the output of the cantilever measured in the uncoupled state. (This is obtained by removing the opposing magnet.) At the resonance frequency, (measured to be approximately 10 Hz) the output of the cantilever exceeds 16 V, and the peak height,

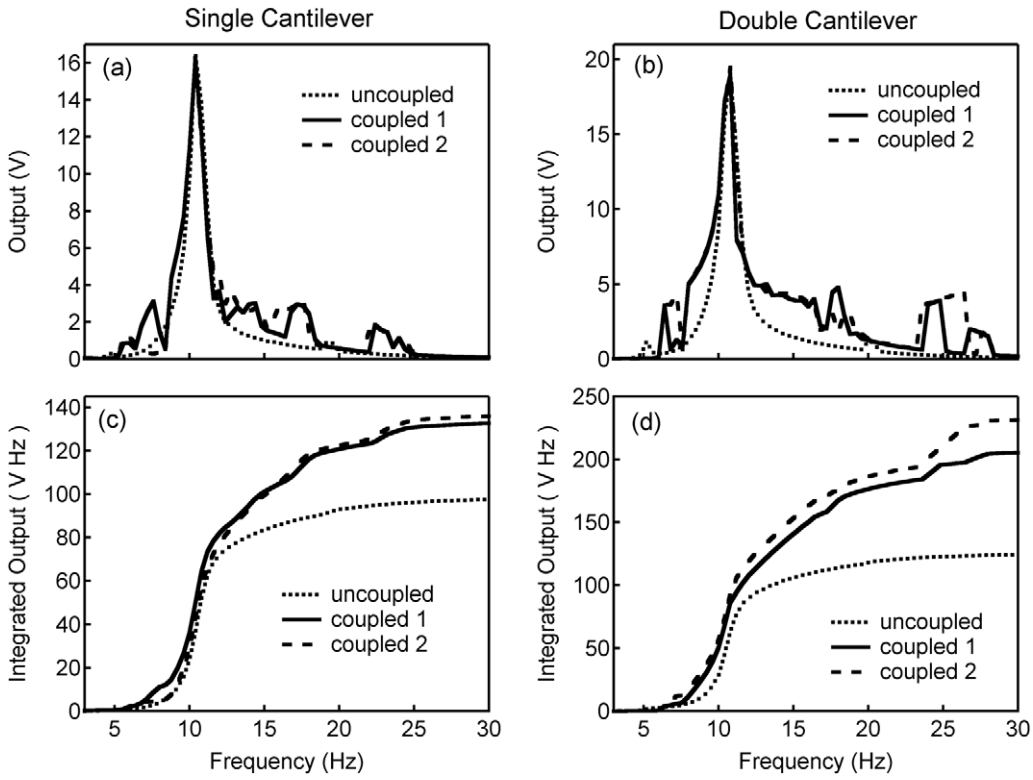

Figure 2. Voltage output of the piezoelectric cantilever as a function of shaker table frequency for (a) single cantilever (b) double cantilever. Integrated voltage output as a function of frequency for (c) single cantilever and (d) double cantilever.

resonance frequency and linewidth are all approximately the same for the coupled and uncoupled states. On either side of the main resonance, however, there is additional output observed for the coupled cantilever, which is not observed in the uncoupled state. As can be seen from a comparison of the two coupled runs, the frequency distribution of the peaks is not completely reproducible, although there is a reproducibility in the overall pattern of the output.

Also measured was a double cantilever system, (as shown in figure 1(c)), in which the second magnet is connected to an opposing cantilever (having resonant frequency of around 60 Hz) rather than to a fixed point. As shown in figure 2(b), the results are similar to the single cantilever system, except that the double cantilever system shows a larger overall increase in off-resonance output. The overall improvement in the harvesting efficiency can be illustrated by plotting the integrated voltage output of the cantilever beam as a function of frequency. For both the single (figure 2(c)) and double (figure 2(d)) cantilever systems, the integrated voltage output over the 0–30 Hz bandwidth shows a substantial increase in the coupled versus the uncoupled case. The total improvement is 31%–87%, with some variation between measurement runs.

Figure 3 shows the output of a single magnetically coupled cantilever measured as a function of time, with the driving frequency in the on-and off-resonance condition. In this case, the voltage output is measured directly across the cantilever. The cantilever used in these experiments was similar to that described in figure 2(a), but had a slightly lower resonant frequency of 10 Hz. At a driving frequency of 7.5 Hz (figure 3(a)) both the uncoupled and coupled cantilever motion follow the vibrations of the shaker table, producing periodic oscillations. The amplitude of the oscillations for the coupled cantilever are larger than those for the uncoupled cantilever, however. At the resonant frequency (figure 3(b)) both coupled and uncoupled cantilevers oscillate at the driving frequency with equal amplitudes. At 13 Hz (figure 3(c)) the uncoupled cantilever motion continues to follow the vibrations of the shaker table, producing low amplitude periodic oscillations. The coupled cantilever motion is aperiodic, however, similar to the chaotic motion observed in a magnetic pendulum [19], with no constant frequency. The results clearly show that above or below the resonant frequency, the magnitude of the coupled cantilever oscillations are appreciably larger than for the uncoupled cantilever, while at resonance, both cantilevers produce the same amplitude voltage.

3. The magnetic forces and spring–mass model

To calculate the amplitude of the cantilever deflection in the presence of the magnetic coupling force in z direction, we use a modified version of the standard spring–mass model [20]. The model parameters are shown schematically in figure 4(a). The cantilever is represented by a one-dimensional spring–mass system, where m is the proof mass, and k is the spring constant. The cantilever deflection, $z(t)$, is driven by a vibrating source, which oscillates sinusoidally with an acceleration A and angular frequency ω. Electrical and mechanical damping are described by the coefficients, b_e and

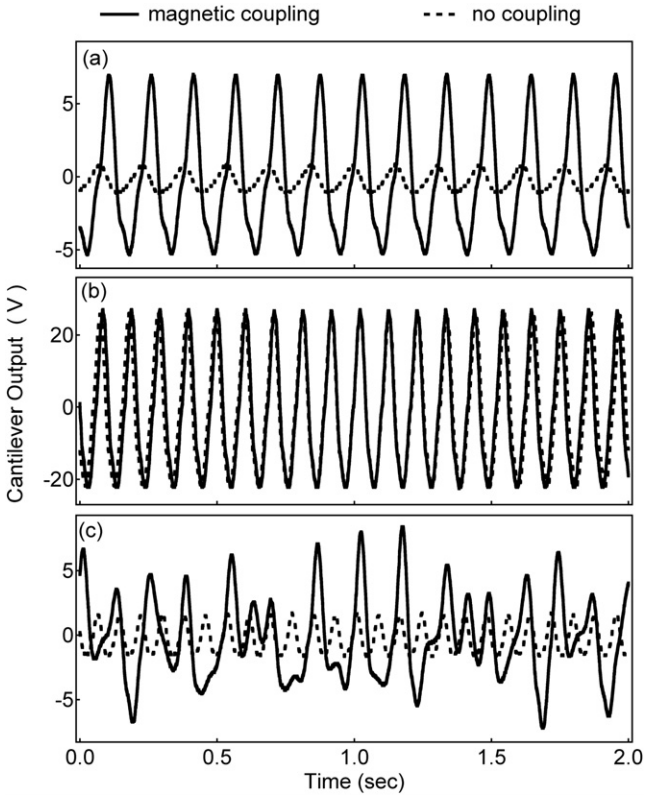

Figure 3. Non-rectified time domain voltage output of the cantilever (a) below resonance, using 6.5 Hz vibration frequency (b) at resonance, using 10 Hz vibration frequency and (c) above resonance, using 13 Hz vibration frequency.

b_{m} respectively. To minimize the complexity of the problem, the magnetic coupling force F_B, is considered to be one-dimensional, acting only in the z-direction, and the magnetic force in the axial direction is ignored (justification for this approximation is provided below). The deflection $z(t)$ can then be determined by solving the differential equation for a one-dimensional forced harmonic oscillator, combined with an unknown non-linear force:

$$\ddot{z}(t) + \frac{b_{\mathrm{e}} + b_{\mathrm{m}}}{m}\dot{z}(t) + \frac{k}{m}z(t) + F_B(z,\eta) = A\cos(\omega t). \quad (1)$$

In general, the magnetic coupling force $F_B(z,\eta)$ is a complicated non-linear function of the deflection z and the magnet/magnet separation distance, η. However, for a given value of η, the force component in the z-direction can be determined experimentally by measuring the weight change of the cantilever under manual deflection. Figure 4(b) shows the experimental set-up for the force determination. The opposing magnet is mounted onto a weighing scale, and the separation between the magnets η is measured at the balance point ($z = 0$) when the magnets are in line with each other. The position of the magnetized cantilever is then manipulated by pushing up and down at the end of a cantilever beam, simulating flexure movement. The deflection z is measured using a micrometer, while the reading on the scale provides the force between the two magnets. The cantilever's restoring force is determined independently by setting the cantilever on the weighing scale, deflecting the cantilever, and recording the weight/deflection relationship.

The magnetic forces $F_B(z,\eta)$ determined for three different magnet separation distances η are plotted in figure 5(a) as a function of the deflection distance z. For all three values of η, two maxima are observed in the magnetic force magnitude, at approximately $z = \pm 5$ mm. This deflection distance is equal to the magnet diameter, and corresponds to the point where the two magnets no longer overlap each other. The magnitude of the maxima increase rapidly with decreasing η. To aid in calculation, the experimentally determined magnetic force values are fit to an empirically determined analytical expression for $F_B(z,\eta)$:

$$F_B(z,\eta) = \frac{az}{(b + cz^4)}, \quad (2)$$

where a, b, and c are fitting parameters. As shown in figure 5(a), this ad hoc expression provides a reasonably accurate fit to the magnetic force data. The influence of the magnetic force can be better appreciated by considering the potential energy of the cantilever as a function of deflection distance, as shown in figure 5(b). The potential energy is determined by integrating over the total force (magnetic force plus restoring force), where the analytical expression for the magnetic force (given by equation (3)) is used. As seen in figure 5(b), the magnetic force modifies the standard harmonic oscillator potential to include two potential minima, one on either side of the zero deflection point, where it is equally likely for the cantilever to lie in either of these minimum points. For large enough magnet separations, motion between the two minima is possible under relatively low amplitude accelerations and at non-resonance driving frequencies.

This discussion ignores the influence of the magnetic force acting along the cantilever axis. To justify this approximation, we also measured the axial force as a function of the cantilever position, using the set-up show in figure 6(a), with the fixed magnet placed perpendicular to the cantilever motion. The results of the measurement are shown in figure 6(b). For a magnet separation of $\eta = 5$ mm, the maximum axial force is 0.044 N at $z = 0$ and drops quickly with distance along the z axis. As described in [12], the resonance frequency of a cantilever under an axial force F is given by:

$$f_{\mathrm{r}}' = f_{\mathrm{r}}\sqrt{1 - \frac{F}{F_{\mathrm{b}}}} \quad (3)$$

where f_{r} is the resonance frequency with no axial force, and F_{b} is the buckling force. The cantilever's buckling force is 0.55 N, obtained from

$$F_{\mathrm{b}} = \frac{\pi^2 EI}{4L^2} \quad (4)$$

where E is the Young's modulus, I is the moment of inertia and L is the length of the cantilever beam. Inserting the appropriate values for our cantilever into the equation above gives a buckling force of 0.55 N which results in a maximum frequency shift of 4.5%. For a resonance frequency of 10 Hz, this results in a frequency shift of 0.45 Hz. In [12], the axial force is much larger, and is kept constant as a function of

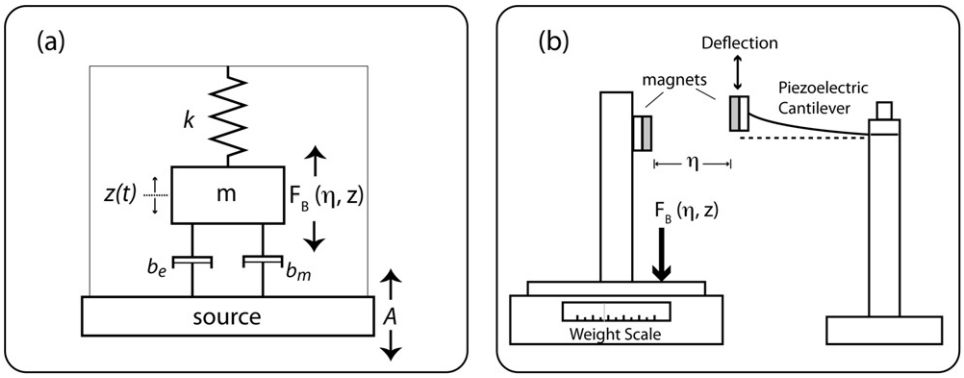

Figure 4. (a) Modified one-dimensional spring force model. A is the source acceleration, k is the spring constant, m is the proof mass, $z(t)$ is the cantilever deflection and $F_B(\eta, z)$ is the magnetic force. (b) Apparatus used to measure the magnetic force $F_B(\eta, z)$.

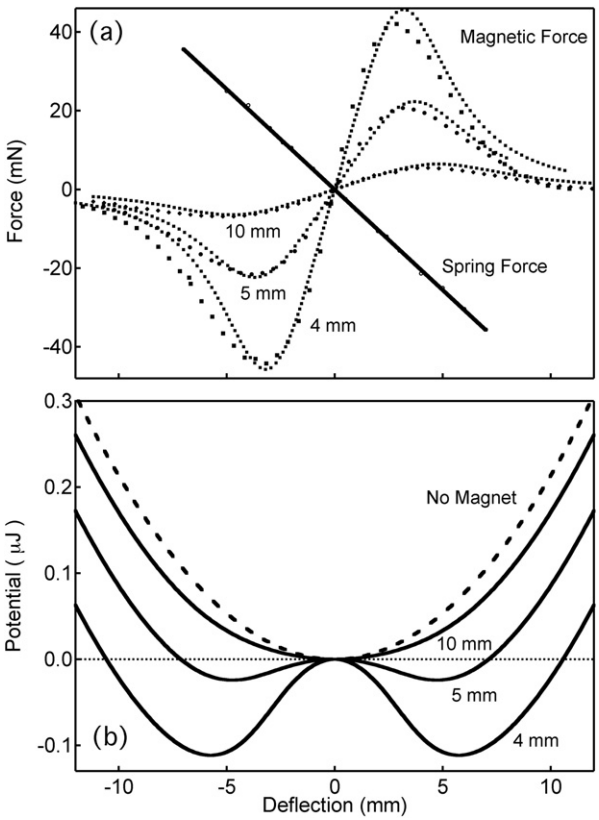

Figure 5. (a) The magnetic force $F_B(\eta, z)$ for three separation distances ($\eta = 4$, 5 and 10 mm). The lines show fits to equation (2). Also shown (as a straight line) is the spring force of the cantilever. (b) The cantilever spring potential (dashed line) and the potential due to the combination of the restoring force and the magnetic force for the three separation distances.

cantilever displacement. In our case, where the axial force drops off with displacement (see figure 6(b)), the frequency shift should be appreciably smaller. These measurements show that the axial force is not a significant factor, making it possible for the cantilever resonance frequency to remain unchanged even in the presence of the magnetic coupling.

Using the analytic expression for the transverse magnetic force (equation (2)), it is now possible to simulate the output of the magnetically coupled cantilever. As described on page 32 in [9], the electrical power produced by a vibrating spring–mass system is given by:

$$P = \tfrac{1}{2} b_e \dot{z}^2 \tag{5}$$

where z is the spring deflection, and b_e is the electrically induced damping coefficient. The instantaneous power at time t is thus proportional to $\dot{z}^2$, which can be determined numerically from equation (1). In our calculation, we evaluate $\dot{z}(t)$ at 0.1 ms time intervals for 2 s and take the average of these values to calculate the time averaged power, normalized by the damping coefficient (P/b_e). Note that the value for the displacement z in this calculation corresponds to the rms value for $z(t)$ rather than the maximum displacement. This is done because the oscillations for the magnetically coupled cantilever are not periodic at all driving frequencies. Figure 7 shows the results of this calculation as a function of driving frequency for both the coupled and uncoupled cantilevers. In the absence of magnetic coupling, a peak in the output is observed at the resonance frequency. With the addition of magnetic coupling, little change is observed in the resonance peak, while non-monotonic fluctuations are observed above and below the resonance frequency. While this is similar to the experimental results, there are also some important differences. The resonance peak in the magnetically coupled output is asymmetric, reducing the above resonance output with respect to the non-coupled case (except near 14 Hz). Also, the theoretical resonant frequency is lower than that observed experimentally. While the specific errors in the model are not known, there are a number of possible reasons why these discrepancies might occur. The calculated solution is averaged over many oscillation periods, and may not capture the chaotic motion of the cantilever fully. Also the calculation does not take into account the fact that each cycle of the response evolves according to the previous cycle history. Both the magnetic and restoring force measurements will have some error (estimated to be approximately 15%) because the three-dimensional magnetic forces are reduced to a one-dimensional force by the scale reading. The discrepancy in the resonant frequency is most likely due to the proof mass distribution around the end of the cantilever, and errors in the spring force measurement.

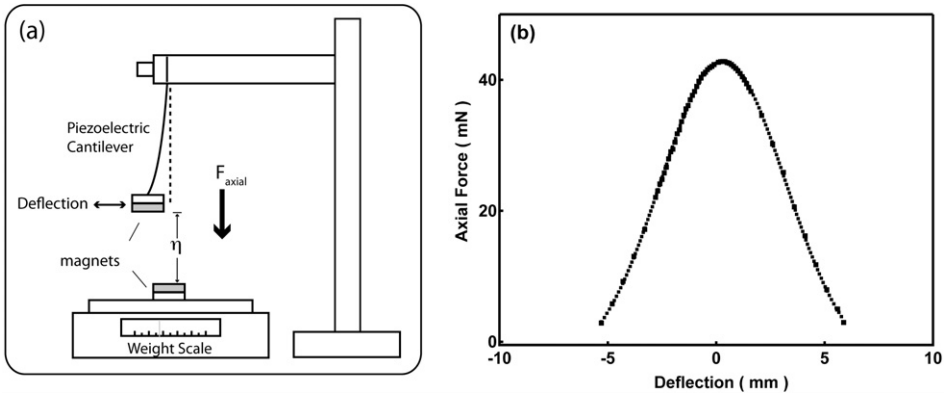

Figure 6. (a) Apparatus used to measure the axial magnetic force. (b) Axial force as a function of deflection distance for a 5 mm separation between the two magnets.

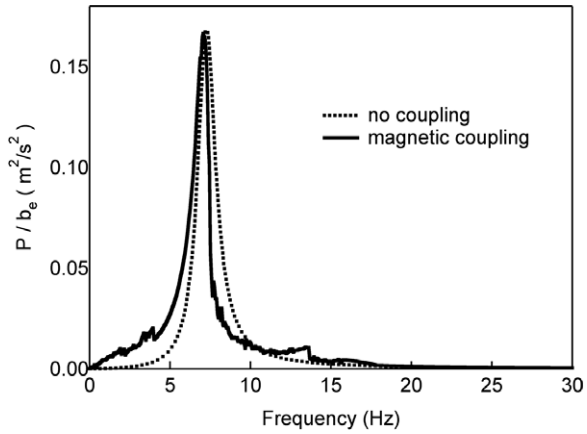

Figure 7. Simulated output of the piezoelectric cantilever for the case of no magnetic coupling (dashed line) and magnetic coupling (solid line).

In contrast to recent experiments in which magnetic coupling is used to modify cantilever motion, we observe no change in the cantilever motion at resonance, (i.e., the resonance frequency remains the same, and the amplitude of the oscillations do not change). We can understand these results by considering the transverse and axial magnetic forces, as measured in figures 5 and 6, respectively. First, in contrast to the situation described in [12], the magnetic forces are much less than the buckling force, and drop off with distance away from the $z = 0$ point. Second, the repulsive force between the two magnets is symmetric, in that there is an equal probability that the cantilever can be deflected up or deflected down, with two local equilibrium points existing on either side of the $z = 0$ point. At the relatively large accelerations that we apply (7 m s^{-2}), the cantilever can be driven beyond the two equilibrium points at resonance. Because the magnetic force drops off rapidly with distance, the modified spring force is approximately the same as the original spring force at the maximum displacement point. From the simulation in figure 7, we determine the maximum displacement to be ± 18 mm. At this distance, the original spring force is 88.2 mN while the modified spring force is 87.4 mN, giving a change of only 0.9%. This results in only a minor change in the resonant frequency. Outside of the resonant frequency, the deflection is smaller, making the magnetic force more important. Off-resonance then, the cantilever undergoes chaotic motion as it moves between the two equilibrium points. By comparison, a single magnet placed above the cantilever as described in [13] and [14], introduces an asymmetric force, which grows in magnitude as the cantilever approaches the magnet. Because the cantilever deflection is largest at resonance, the influence of the magnetic force is particularly large at the resonance frequency, and damping is observed.

4. Conclusions

Piezoelectric cantilevers have been widely studied for energy harvesting applications, but suffer from poor output power outside of a narrow frequency range near the cantilever resonance. In this study, we have demonstrated how power output can be enhanced by applying a simple repulsive magnetic force to a piezoelectric cantilever beam to compensate the cantilever spring force, and lower the restoring potential on either side of the equilibrium point. For a symmetric magnetic force, the cantilever's resonant frequency and amplitude at the resonant frequency does not alter, however, there is an increase in the off-resonance output. The dynamic between the magnetic and spring forces increases the total voltage generated by the electric cantilever across the scanned frequency spectrum. The principle may be generally applied to improve the integrated voltage output of any energy harvesting system that works by scavenging mechanical vibrations.

Acknowledgments

The effort was funded by the Department Of Energy DE-FC26-06NT42795 and US Navy under Contract DAAB07-03-D-B010/TO-0198. Technical program oversight under Navy contract was provided by Naval Surface Warfare Center, Crane Division.

Disclaimer

This report was prepared as an account of work sponsored by an agency of the United States Government. Neither the

References

[1] Elvin N G, Elvin A and Choi D 2003 A self-powered damage detection sensor *J. Strain Anal. Eng. Des.* **38** 115–24

[2] Ottman G K, Hofmann H F and Lesieutre G A 2003 Optimized piezoelectric energy harvesting circuit using step-down converter in discontinuous conduction mode *IEEE Trans. Power Electron.* **18** 696–703

[3] Roundy S 2004 A piezoelectric vibration based generator for wireless electronics *Smart Mater. Struct.* **13** 1131

[4] Kulah H and Najafi K 2004 An electromagnetic micro power generator for low-frequency environmental vibrations *MEMS'04: 17th IEEE Int. Conf. on Micro Electro Mechanical System* pp 237–40

[5] von Büren T and Tröster G 2007 Design and optimization of a linear vibration-driven electromagnetic micro-power generator *Sensors Actuators* A **135** 765–75

[6] Beeby S P, Torah R N, Tudor M J, Glynne-Jones P, O'Donnell T, Saha C R and Roy S 2007 A micro electromagnetic generator for vibration energy harvesting *J. Micromech. Microeng.* **17** 1257–65

[7] Lo H-w and Tai Y-C 2008 Parylene-based electret power generators *J. Micromech. Microeng.* **18** 104006–14

[8] Sterken T, Fiorini P, Baert K, Puers R and Borghs G 2003 An electret-base electrostatic micro-generator transducers *The 12th IEEE Int. Conf. on Solid State Sensors, Actuators and Microsystems (Boston, June)* pp 1291–4

[9] Roundy S, Wright P K and Rabaey J M 2004 *Energy Scavenging for Wireless Sensor Networks with Special Focus on Vibrations* (Norwell, MA: Kluwer Academic Publishers)

[10] Chiu Y and Tseng V F G 2008 A capacitive vibration to electricity energy converter with integrated mechanical switches *J. Micromech. Microeng.* **18** 104004–12

[11] Leland E S and Wright P K 2006 Resonance tuning of piezoelectric vibration energy scavenging generators using compressive axial preload *Smart Mater. Struct.* **15** 1413–20

[12] Zhu D, Roberts S, Tudor M J and Beeby S P 2008 Closed loop frequency tuning of a vibration-based microgenerator *Proc. PowerMEMS 2008/MicroEMS2008 (Nov. 2008)* pp 229–32

[13] Challa V R, Prasad M G, Shi Y and Fisher F T 2008 A vibration energy harvesting device with bidirectional resonance frequency tunnablity *Smart Mater. Struct.* **17** 015035

[14] Lin J-T, Jones W, Alphenaar B, Xu Y and Alphenaar D 2008 Passive magnetic coupling for enhanced piezoelectric cantilever response for energy scavenging applications *ISAF 2008 EH017: 17th Int. Symp. on Applications of Ferroelectrics (Feb. 2008)* EH017

[15] Roundy S and Zhang Y 2005 Toward self-tuning adaptive vibration-based microgenerator *Smart Structure, Devices and System II*; *Proc. SPIE* **5649** 373–84

[16] Cottone F, Vocca H and Gammaiton L 2009 Non-linear energy harvesting *Phys. Rev. Lett.* **102** 080601

[17] Erturk A, Hoffmann J and Inman D J 2009 A piezomagnetoleastic structure for broadband vibration energy harvesting *Appl. Phys. Lett.* **94** 254102

[18] Staton S C, Mcgehee C C and Mann B P 2009 Reversible hysteresis for broadband magnetopiezoelastic energy harvesting *Appl. Phys. Lett.* **95** 174103

[19] Siahmakoun A, French V A and Patterson J 1997 Nonlinear dynamics of a sinusoidally driven pendulum in a repulsive magnetic field *Am. J. Phys.* **65** 393–400

[20] Williams C B and Yates R B 1996 Analysis of a micro-electric generator for microsystems *Sensors Actuators* A **52** 8–11